

Application of Local Point Interpolation Method to Electromagnetic Problems with Material Discontinuities using a new Visibility Criterion

Naïsses Z. Lima¹, Alexandre R. Fonseca², Renato C. Mesquita¹

¹Department of Electrical Engineering – Universidade Federal de Minas Gerais

²Department of Computing – Universidade Federal dos Vales do Jequitinhonha e Mucuri

naisseszoia@gmail.com, renato@ufmg.br, arfonseca@ufvjm.edu.br

Abstract — In this paper the Local Point Interpolation Method (LPIM) is used with a modified visibility criterion to handle material discontinuities. In general, visibility criterion is applied only to shape function generation. We present a modified version where it is also applied to the integration process. The method is simpler and more robust than other techniques often employed on multi-materials problems, with a straightforward implementation.

I. INTRODUCTION

Meshless methods are numerical techniques to solve boundary value problems [1]. They were developed with the goal of eliminating the need of mesh generation, working only with nodes without a prescribed connectivity among them [1].

In this paper we use the Local Point Interpolation Method (LPIM) [1]. LPIM works with local weak forms and uses the Point Interpolation Method (PIM) to build its shape functions, which satisfy the Kronecker delta property, i.e., the boundary conditions are easily imposed [1].

Most of the work done so far with LPIM is limited to problems dealing with one material, as we can see in [1], or problems with simple geometry formed by two materials handled by a single interface. Besides that, we do not see in literature multiple materials problems with sources terms. As it can be seen in [2]-[3], material discontinuity can be treated by enforcing conditions on the potential and its normal derivative using duplicated points and a collocation method. Reference [4] adds a special jump function as a shape function to reproduce the discontinuous behavior. In [5] the interface problem is dealt applying the visibility method on the shape functions, meaning that nodes are used to compute shape functions only for their own material or for the surrounding interface.

We present a different approach for dealing with the problem: a visibility method on both shape function construction and integration process. With this technique we are able to solve problems of multiple materials, interfaces and existing sources terms. As will be seen, the method is more robust, especially when compared to collocation methods, and also simpler, once there is no need to use special shape functions neither to duplicate nodes.

II. LOCAL POINT INTERPOLATION METHOD

Magnetostatic problems in 2D can be described by

$$\nabla \cdot (\nu \nabla A) = -J_z \quad (1)$$

where ν is the magnetic reluctivity, J_z is the current density and A is the magnetic vector potential z-component. Boundary conditions are given by (2) on Dirichlet boundary

Γ_g , Neumann boundary Γ_h and on the interface Γ_I between materials.

$$A = g \text{ on } \Gamma_g, \quad -\nu \frac{\partial A}{\partial n} = h \text{ on } \Gamma_h, \quad \nu_1 \frac{\partial A_1}{\partial n} = \nu_2 \frac{\partial A_2}{\partial n} \text{ on } \Gamma_I. \quad (2)$$

A local weak form can be obtained for each quadrature domain Ω_q^i (Fig. 1)

$$\begin{aligned} - \int_{\Omega_q^i} \nu \nabla w_i \cdot \nabla A d\Omega + \int_{\Gamma_{q \cup qg}^i} w_i \nu \frac{\partial A}{\partial n} d\Gamma \\ = - \int_{\Omega_q^i} w_i J_z d\Omega + \int_{\Gamma_{qh}^i} w_i h d\Gamma. \end{aligned} \quad (3)$$

Petrov-Galerkin formulations allow the use of shape and test functions belonging to different spaces. We choose Heaviside step test functions and the first integral over domain vanishes. The resultant local equation is

$$\int_{\Gamma_{q \cup qg}^i} \nu \frac{\partial A}{\partial n} d\Gamma = - \int_{\Omega_q^i} J_z d\Omega + \int_{\Gamma_{qh}^i} h d\Gamma. \quad (4)$$

The PIM shape functions are generated using radial and polynomial basis functions (RPIMp). Once they satisfy the Kronecker delta property, Dirichlet boundary conditions are easily enforced [1].

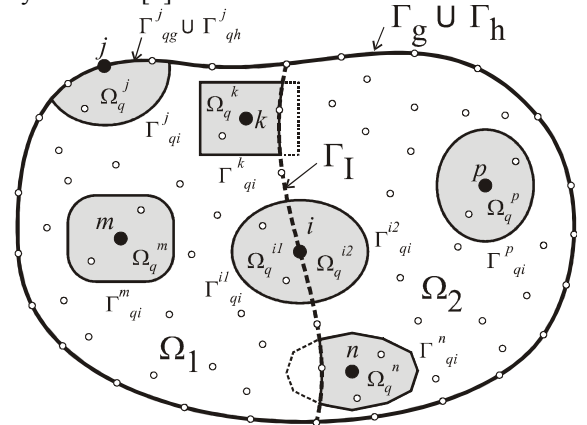


Fig. 1. Domain representation Ω with boundary Γ . $\Omega = \Omega_1 \cup \Omega_2$. Γ is the union of Dirichlet (Γ_g), Neumann (Γ_h) and interface (Γ_I) boundaries. For a quadrature domain Ω_q^i defined for node i , Γ_q^i is the union of Dirichlet (Γ_{qg}^i), Neumann (Γ_{qh}^i), internal (Γ_{qi}^i) and interface (Γ_{qi}^i) boundaries.

III. TREATING MATERIAL DISCONTINUITIES

Consider a domain with two different materials separated by the interface Γ_I as shown in Fig. 1. To apply the visibility criterion we first split all nodes into three sets: S_1 , S_2 and S_I , where S_1 contains all the nodes that belong exclusively to region 1 (e.g. nodes j , m , k), S_2 contains the nodes belonging exclusively to region 2 (e.g. nodes n , p) and S_I is a set containing the nodes lying on Γ_I (e.g. node i).

For shape function construction the procedure is the same as in [1]. The support domain of a point from region 1 contains nodes from S_1 and S_l . Similarly, the support domain of a point from region 2 contains nodes from S_2 and S_l . Finally, the support domain of a point on Γ_l contains nodes from S_1 , S_2 and S_l .

For the local weak form integration, if we are integrating over a local domain of a node from S_1 , only the geometry corresponding to region 1 is used. Γ_l is considered as an internal boundary and the integration follows (4). For node k , for example, the resulting local domain is as shown in Fig. 1 and all the local boundaries are considered internal. The same idea is applied in region 2.

A node i at Γ_l has local quadrature domain in both regions 1 and 2, as in Fig. 2, and Γ_l is considered separately. For regions 1 and 2, we have, respectively, (5) and (6).

$$\int_{\Gamma_{q1}^{i1}} v_1 \frac{\partial A}{\partial n} d\Gamma + \int_{\Gamma_{q1}^{i1}} v_1 \frac{\partial A_1}{\partial n_1} d\Gamma = - \int_{\Omega_q^{i1}} J_z d\Omega + \int_{\Gamma_{q1}^{i1}} h d\Gamma. \quad (5)$$

$$\int_{\Gamma_{q2}^{i2}} v_2 \frac{\partial A}{\partial n} d\Gamma + \int_{\Gamma_{q2}^{i2}} v_2 \frac{\partial A_2}{\partial n_2} d\Gamma = - \int_{\Omega_q^{i2}} J_z d\Omega + \int_{\Gamma_{q2}^{i2}} h d\Gamma. \quad (6)$$

As we are integrating the whole local domain, we have to add (5) and (6). As the interface boundary is the same for both domains ($\Gamma_{q1}^{i1} = \Gamma_{q2}^{i2}$), $\vec{n}_1 = -\vec{n}_2$, and the RPIMp shape functions possess the Kronecker delta property, from (2) the two integrals for Γ_{q1}^{i1} and Γ_{q2}^{i2} are cancelled. The final expression for the interface node local quadrature domain is

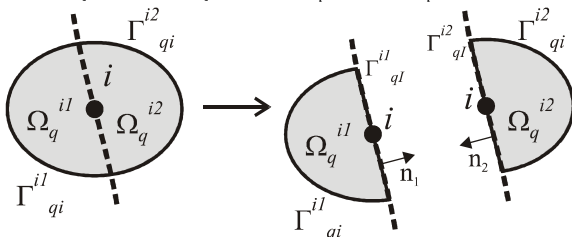
$$\begin{aligned} \int_{\Gamma_{q1}^{i1}} v_1 \frac{\partial A}{\partial n} d\Gamma + \int_{\Gamma_{q2}^{i2}} v_2 \frac{\partial A}{\partial n} d\Gamma = \\ - \int_{\Omega_q^{i1}} J_z d\Omega - \int_{\Omega_q^{i2}} J_z d\Omega + \int_{\Gamma_{q1}^{i1}} h d\Gamma + \int_{\Gamma_{q2}^{i2}} h d\Gamma. \end{aligned} \quad (7)$$


Fig. 2. Local integration domain for a node i at interface. Visibility criterion is applied splitting domain Ω_q^i into two: one belonging to region 1 (Ω_q^{i1}) and the other belonging to region 2 (Ω_q^{i2}).

IV. NUMERICAL RESULTS AND CONCLUSIONS

An electromagnet problem is solved using the discussed technique. The implementation is held by the framework presented in [6]. The relative magnetic reluctivities are $\nu_{air} = \nu_{copper} = 1$ and $\nu_{iron} = 10^{-3}$. The current density is $J_z = 10^{-1}$ (MA/m²). Fig. 3 shows the LPIM solution using 1288 nodes evenly distributed, 4 integration points for boundary integration and 1 integration point for domain integration. Rectangular quadrature domains and linear polynomials with cubic spline radial basis function [1] for RPIMp are used.

The convergence rate is also investigated using four sets of different nodes distribution. The result is compared to FEM approximation (Fig. 4). The reference solution for

computing the error norm is the FEM solution with 10^6 nodes. Both methods have almost the same convergence rate (1.39 for LPIM and 1.34 for FEM) and LPIM achieves more accurate solution than FEM.

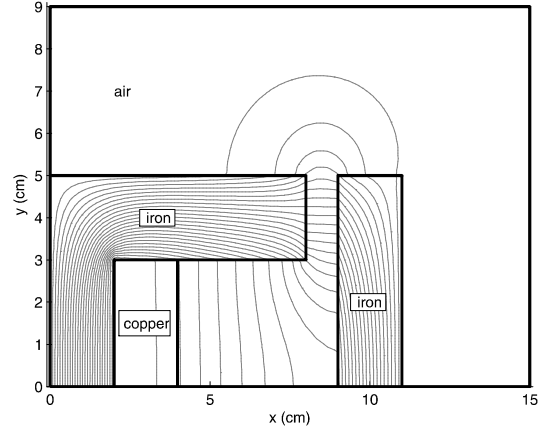


Fig. 3. Magnetic vector potential distribution evaluated by LPIM.

Concluding, we can say that the new visibility technique to handle material discontinuities in LPIM is robust since it works with integration around interfaces. Its implementation is also very simple, since there is no need to duplicate nodes.

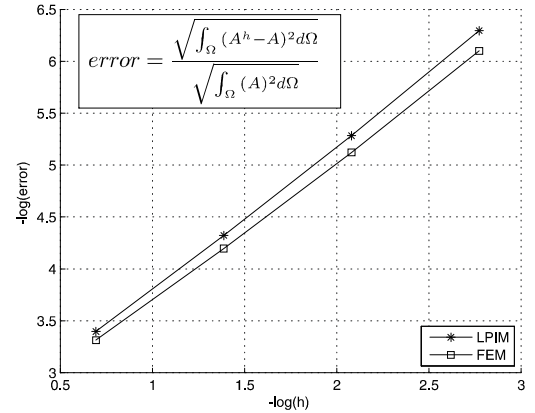


Fig. 4. Error norm for LPIM with RPIMp shape function and for FEM. h is the distance among nodes. A is the reference solution and A^h is the approximated numerical solution.

V. REFERENCES

- [1] G. R. Liu, *Meshfree Methods – Moving Beyond the Finite Element Method*, CRC Press, 2nd ed., 2009.
- [2] Q. Li, S. Shen, Z. Han, and S. Atluri, *Application of Meshless Petrov-Galerkin (MLPG) to Problems with Singularities, and Material Discontinuities, in 3-D Elasticity*, CMES, vol. 4, no. 5, pp. 571-585, 2003.
- [3] W. L. Nicomedes, R. C. Mesquita, F. J. S. Moreira, "A Meshless Local Boundary Integral Equation method for three dimensional scalar problems," *CEFC 2010*, May 2010.
- [4] L. Huifen and J. Hao, "Application of meshless local Petrov-Galerkin methods in electromagnetics," *ICEMS 2003*, pp. 798-801, Nov. 2003.
- [5] S. A. Viana, D. Rodger, H. C. Lai, "Meshless local Petrov-Galerkin method with radial basis functions applied to electromagnetics," *IEE Proceedings Science, Measurement and Technology*, vol. 151, no. 6, pp. 449-451, 2004.
- [6] N. Z. Lima, R. C. Mesquita, M. L. A. Junior, "A framework for meshless methods using generic programming", *CEFC 2010*, May 2010.